

Load Resistance Influence of Magnetolectric Characteristics on NiZnFe₂O₄+PZT Composites for Magnetolectric Sensors

Ji-Goo Ryu⁺ and Su-Tae Chung

Abstract

The influences of the load resistance R_L on the magnetolectric (ME) characteristics of NiZnFe₂O₄+PZT composite were investigated in the non-resonance frequency range. The ME coefficient peak increases with increasing R_L , but the frequency indicating the ME coefficient peak decreases with increasing R_L . The maximum output power peak is approximately 9.3×10^{-10} mW/Oe near $R_L=3.3$ M Ω at $f=280$ Hz, and the ME coefficient seems to be saturated at $R_L>20$ M Ω . This frequency shift effect of R_L shows that the frequency range for an ME sensor application can be modulated with the appropriate value of R_L . The ME output voltage has a good linear response to the ac field H_{ac} and shows fair stability over a range of temperatures. The measured non-linearity of this sample is approximately 0.8%. This sample will allow for a low-strength magnetic ac-field sensor. The result from this sample will serve as basic data for a signal-processing circuit system.

Keywords : Magnetolectric sensor, Magnetolectric effect, Electromechanical, Magnetostriction coefficient, Load resistance

1. INTRODUCTION

The action of a magnetolectric (ME) sensor is based on magneto-electric interaction. The ME effect is defined as a variation of electric polarization in a system as a response to an applied magnetic field, or an induced magnetization by an external electric field [1, 2]. An applied magnetic field produces deformation in ferrite due to magnetostriction and results in an induced electric polarization due to the piezoelectric effect in ferroelectric phase.

The ME effect shows a variety of device applications including magnetic field sensors, data storage devices, actuators and transducers [3, 4].

The ME effect was observed in single-phase materials, two-phase bulk composites and two or three, multilayered composites [4-8]. In these structures, the ME coefficient of the layered composites is considerably higher than that observed in bulk composites. However, the bulk

composites have several advantages over layered composites, such as easy and cheap fabrication, good mechanical strength, and ME parameter modulation with a proper choice for the two phases. Bulk composites using the conventional ceramic method have been widely studied because of their advantages [5, 9-12].

Therefore, we choose a NiZnFe₂O₄+PZT composite system known as a ferrite phase (NiZnFe₂O₄) having high magnetostriction and a ferroelectric phase (PZT) having high electromechanical coupling [13, 14]. The study on the influences of the load resistance of ME characteristics requires the use of a practical ME sensor. Recently, research groups have focused on the influence of the load resistance R_L to enable ME sensor applications, and their research has been performed in other ME materials [15-17]. However, the research on the influence of the load resistance on the NiZnFe₂O₄+PZT composite has not yet been comprehensively conducted.

In this paper, the samples were prepared by the conventional ceramic method and the influence of R_L on the ME characteristics is investigated in the non-resonance frequency range.

2. EXPERIMENTAL

2.1 Preparation of ME composite sample

Department of Electronic Engineering, Pukyong National University, Busan, Korea

599-1, Daeyeon 3-Dong, Nam-Gu, Busan, Korea

⁺Corresponding author: ryujg@pknu.ac.kr

(Received : Jul. 11, 2013, Revised : Aug. 28, 2013, Accepted : Aug. 29, 2013)

This is an Open Access article distributed under the terms of the Creative Commons Attribution Non-Commercial License (<http://creativecommons.org/licenses/by-nc/3.0>) which permits unrestricted non-commercial use, distribution, and reproduction in any medium, provided the original work is properly cited.

Piezoelectric material and ferrite material were prepared by a conventional solid-state reaction method in air. Reagent-grade powder, PbO, ZrO₂, TiO₂, NiO, ZnO, Nb₂O₅ and Fe₂O₃ were used as raw materials.

For the preparation of PE[0.5Pb(Zr_{0.4}Ti_{0.6})O₃-0.25Pb(Ni_{1/3}Nb_{2/3})O₃-0.25Pb(Zn_{1/3}Nb_{2/3})O₃:piezoelectric material], we used the columbite precursor method so as to obtain a stabilized perovskite structure [20].

We first prepared the columbite-structure NiNb₂O₆ and ZnNb₂O₆, which were synthesized by calcining mixtures of NiO and ZnO with Nb₂O₅ at 1,100°C for 4 hours, respectively. The precursor materials were then mixed in stoichiometric ratios with PbO, ZrO₂, and TiO₂. The mixed powder was dried and calcined at 900°C for 4 hours in a sealed MgO crucible [21].

For the preparation of PM [(Ni_{0.9}Zn_{0.1})Fe₂O₄: ferrite material], a stoichiometric mixture of NiO, ZnO, and Fe₂O₃ was dried and calcined at 1,000°C for 5 hours in an Al₂O₃ crucible. Particulate magnetoelectric ceramic composites were prepared by a conventional solid-state reaction method using the above synthesized piezoelectric and ferrite materials according to the formula (1-x) PE-xPM (x=0.1, 0.15, 0.2).

The pellet formation was accomplished with a cold pressure of 1,000 kg/cm². The pellets were sintered at 1,200°C for 2 hours in a sealed MgO crucible. The sample was cut and polished to have a rectangular shape (4×7 mm², thickness 1 mm), and the sample surface was coated with a thin layer of silver paste as electrodes. The samples were electrically poled along the direction of the thickness. The electric polling was conducted by applying an electric field of 1.8 kV/mm at 100°C for 20 min in silicon oil.

Fig. 1 shows the SEM microstructure of ME samples with (1-x) PE-xPM composites (x=0, 0.2, 1).

Table 1 lists the results of EDX analysis of a large grain (#1) and a small grain (#2) in the sample with x=0.2.

In the sample shown in Fig. 1(a), the PE phase shows large granules and density, and the grain size was approximately 1.72 μm. However, in the sample shown in Fig. 1(c), the PM phase shows small granules and few pores and the grain size was 0.7 μm. The sample in Fig. 1 (b) clearly exhibits two distinct phases: the PE phase with large grains and the PM phase with small grains. We confirmed that the composites were formed in either 0-3 or 3-0 modes with PE and PM phases as classified by G. Harshe [22]. The grain size of the PE phase in multiphase composite was smaller than that of the homogeneous PE

phase. The grain growth of the PE phase decreases because of the existence of ion diffusion in grain boundaries as shown Table 1.

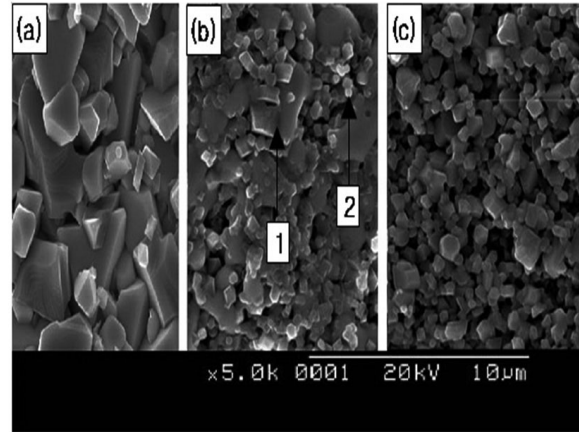


Fig. 1. SEM micrographs of the (1-x) PE - x PM composites; (a) x=0, (b) x=0.2, 1: PE phase, 2: PM phase, and (c) x=1

Table 1. Chemical composition of different grain of the 0.8PE-0.2PM composites obtained by EDX analysis.

Element	PE (#1)		PM (#2)	
	wt%	mol%	wt%	mol%
O	20.3	66.7	26.8	62.2
Ti	3.4	3.7	4.3	3.3
Fe	2.5	2.4	28.5	16.2
Ni	1.2	1.1	20.7	10.5
Zn	1.1	0.9	5.7	3.2
Zr	3.5	2.0	3.6	1.6
Nb	18.9	10.7	4.6	1.9
Pb	49.1	12.5	5.8	1.0

Table 2. Physical properties of the (1-x) PE - xPM particulate ceramic composites

x	D (g/cm ³)	S (S/cm)	ε _r	tan δ
0	7.93	1.68 × 10 ⁻¹¹	2138	0.0267
0.1	7.54	1.99 × 10 ⁻¹⁰	1850	0.0264
0.2	7.35	1.23 × 10 ⁻¹⁰	1576	0.0274

Table 2 shows the conductivity, dielectric constant and dielectric loss in (1-x) PE-xPM composites (x=0, 0.1, 0.2). The dielectric constant of the composites decreased, and

the conductivity and dielectric loss increased with increasing PM phase. This is due to the high conductivity of ferrite material.

2.2 Measurements

The ME effect in the composition was measured with the set-up shown in Fig. 2. The magnetoelectric coefficient (dE/dH_{ac}) was measured by applying an ac magnetic field with a frequency in the range of 10 Hz ~ 10 kHz and an amplitude $H_{ac}=1$ Oe under dc magnetic bias ($H_{dc}=0\sim 7$ kOe). The ac magnetic field H_{ac} was generated by a Helmholtz coil, and the output voltage generated from the ME sample was measured using an SRS lock-in amplifier (model SR 830).

The ME coefficient is obtained as follows

$$\alpha_E = \frac{U}{d \times H_{ac}} \quad (1)$$

Where U , d and H_{ac} are the ME voltage, the effective thickness of the sample, and the amplitude of the ac magnetic field, respectively.

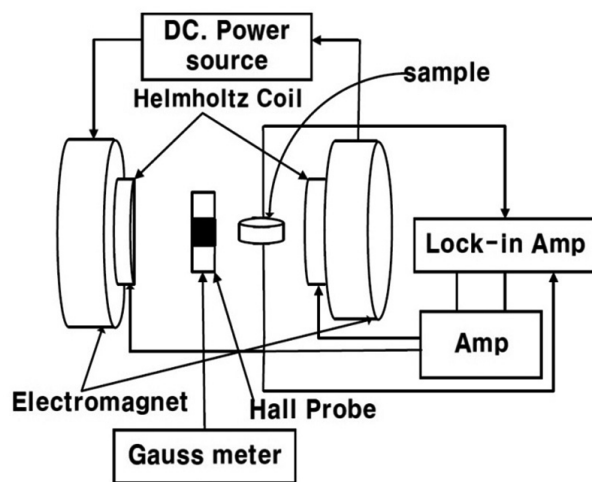


Fig. 2. Schema of experimental set-up.

The schema showing the ME transverse (PE perpendicular to H) and longitudinal (PE parallel to H) measurement is presented in Fig. 3. All measurements were carried out at room temperature and atmospheric pressure without unnecessary external magnetic fields. The

measurement of the ME voltage was performed for two different magnetic field orientations with respect to the electrical polarization PE to obtain the transverse and longitudinal ME voltage coefficients.

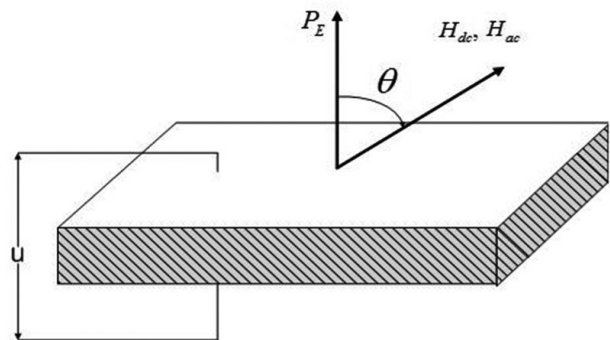


Fig. 3. Schema of the longitudinal and transverse ME coefficient measurements.

3. RESULTS AND DISCUSSIONS

Fig. 4 shows the dependence of the longitudinal and transverse magnetoelectric (ME) coefficients as a function of the dc bias field H_{dc} . Measurement were performed on the NZFO sample with $x=0.2$ at an ac field $H_{ac}=1$ Oe and $f=100$ Hz. The maximum ME coefficient of this sample was obtained at 0.2NZFO+0.8PZT as ref. [20]. The longitudinal ME coefficient increased with H_{dc} , but the transverse ME coefficient decreased.

The magnitudes of the longitudinal and transverse ME coefficients reached a maxim of 27.8 mV/Oe.cm at $H_{dc}=780$ Oe, and 15.7 mV/Oe.cm at $H_{dc}=380$ Oe, respectively. Further increasing H_{dc} leads to a reduction in the ME coefficient. The longitudinal ME coefficient was larger than the transverse coefficient. Such an H_{dc} -dependence of the ME coefficient was due to the change of the magnetostriction λ [21]. The ME coefficient reaches its maximum value at the bias magnetic fields corresponding to the peak value in the piezomagnetic coupling $q=d\lambda/dH_{dc}$ [21, 22]. When changing the measuring condition from the transverse type to the longitudinal type, H_{max} ranged from 380 to 780 Oe. The field of the longitudinal type was approximately twice as large as that of the transverse type. Here, H_{max} denotes the H_{dc} of the maximum ME coefficient.

The change in H_{max} between the longitudinal and

transverse types is due to the different demagnetizing field and the different piezomagnetic coupling associated with the field orientation [23, 24]. For this sample, the output signal linearly increased when increasing the bias static field H_{dc} at $f=100$ Hz and reached its maximum value near $H_{dc}=780$ Oe (longitudinal type).

This point will allow for application to low-magnetic field sensors, even though the ME coefficient is smaller than that of the layered ME devices [4, 25].

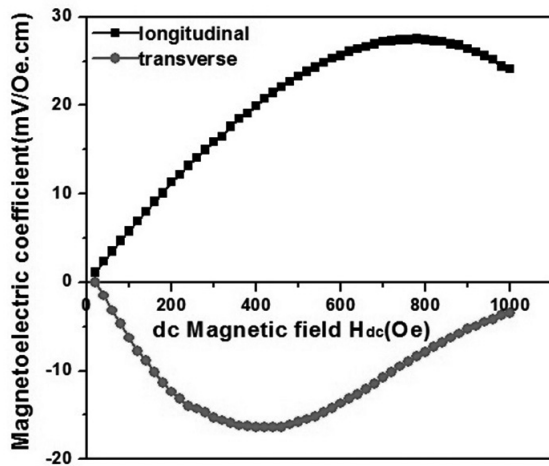


Fig. 4. Dependence of the magnetolectric coefficient vs. bias static magnetic field at $f=100$ Hz.

Fig. 5 shows the ME voltage measured under different magnetic field (H_{ac} , H_{dc}) directions with respect to electrical polarization PE (i.e: with different angle θ) as shown in Fig. 3. Measurements were performed for H_{dc} set at $H_{ac}=1$ Oe and $f=100$ Hz. The ME voltage U decrease with increasing angle θ and exhibits a complex variation in both magnitude and sign. Ultimately, a complete change in its sign is found at $\theta=\pi/2, \pi/3$.

The different sign of the ME voltage is related to the different strain in the PZT phase. Generally, for an angle in the range of $0<\theta<\pi/2$, the external magnetic field can be revealed as a sum of two components perpendicular and parallel to the electrical polarization PE direction: $H = H_{\parallel} + H_{\perp} = H \cos \theta + H \sin \theta$ [26].

Hence, the sign of the ME voltage will depend on the competition between these two magnetic field components (also at Fig. 4). The action of H_{\parallel} contributes to a positive ME voltage, whereas that of H_{\perp} causes a negative voltage. Therefore, a practical sensor must have $\theta=0$ (i.e: longitudinal).

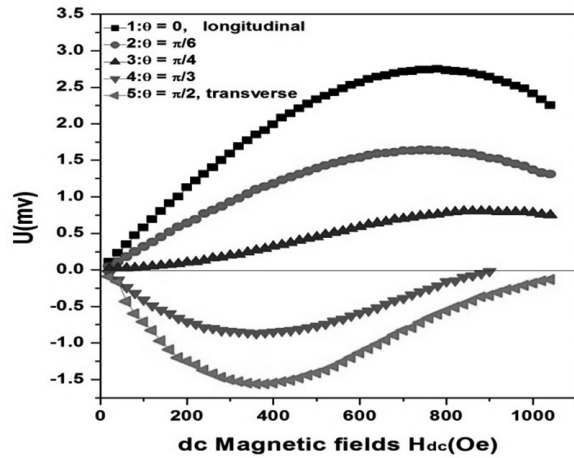


Fig. 5. ME voltage measured at different directions between electrical polarization PE and H_{dc} , H_{ac} field.

Fig. 6 shows the dependence of the ME coefficient vs. the frequency of ac magnetic field under bias static magnetic fields corresponding to the maximum ME coefficient for each sample (NZFO: $x=0.1, 0.15, 0.2$, longitudinal type). Measurements were performed under optimal maximum bias static fields and ac field $H_{ac}=1$ Oe. For all the samples, the maximum ME coefficient was observed near the ac field frequency $f=100$ Hz. The ME coefficient increased with NZFO content and the maximum ME coefficient was obtained with the 0.2NZFO+0.8PZT sample at $f=100$ Hz. The optimum frequency of this sample was near $f=100$ Hz. This frequency is not the resonant frequency because it is quite low compared to those reported in ref. [7]. This low-frequency behavior has been observed earlier for the NZFO-PZT and NFO-PZT system [7, 27].

The decrease in ME coefficient in the frequency region of (10 Hz ~ 2 kHz) is due to the conductivity of ferrite and the piezoelectric phase [23]. The conductivity results in an undesirable leakage of charge in the piezoelectric phase. Namely, the discharge process occurs through the sample resistance [24].

Fig. 7 shows the frequency dependence of the ME coefficient for the 0.2NZFO+0.8PZT sample at an ac field $H_{ac}=1$ Oe, an optimal bias static field $H_{dc}=780$ Oe, and various load resistance R_L (including the open-circuit condition). The previous research on the influence of the load resistance was also observed in other ME materials [15-17].

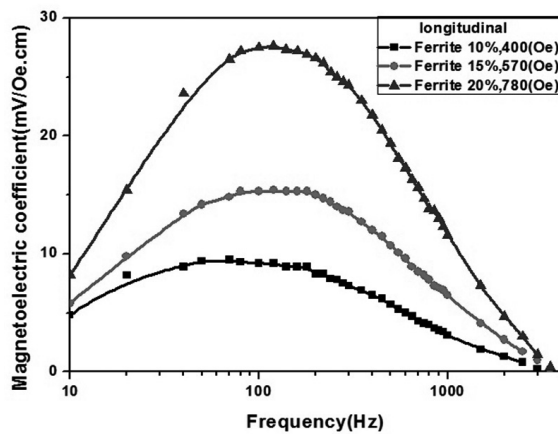


Fig. 6. Magnetoelectric coefficient vs. frequency of ac magnetic field.

This research has been investigated in the resonance frequency range, but our research was mainly performed on the characteristics of the ME sample in the non-resonance frequency range (10 Hz ~ 7 kHz). In the low-frequency range, the ME coefficient decreases with decreasing frequency f for various R_L , and the cut-off frequency (f_{cut}) decreases with increasing R_L . As Hac is sinusoidal wave, f_{cut} can be expressed as $f_{cut} = 1/2\pi\tau$, where $\tau = RC$ is the time constant, C is the capacitance of the piezoelectric phase and R is the parallel resistance of the composites resistance (R_C), the input resistance (R_E) of the electrometer, and the R_L . Here, R can be approximately set to R_L because R_L is smaller than R_C and R_E [16, 28].

Therefore, R increases with increasing R_L . In the frequency range of 10 Hz to 7 kHz, the maximum ME coefficient is shown under the open-circuit condition and is approximately 27.8 mV/Oe.cm as shown in Fig. 6.

In the frequency range of 100 Hz to 7 KHz, the ME coefficient peak value gradually increased with increasing R_L , but the frequency indicated that the ME coefficient peak values decreased with increasing R_L .

The reason for the frequency shift to the higher frequency and the decrease of the ME coefficient peak values caused by decreasing R_L can be explained by the impedance matching condition and $f_{cut} = 1/2\pi R_L C$. Namely, if the internal impedance of this sample most likely consists of the capacitor component (PZT), impedance matching will occur when the impedance magnitude $1/2\pi f_{cut} C$ of this sample is approximately equal to R_L . The decrease in the ME coefficient peak caused by decreasing R_L is likely due to the voltage drop in the internal resistance of this sample.

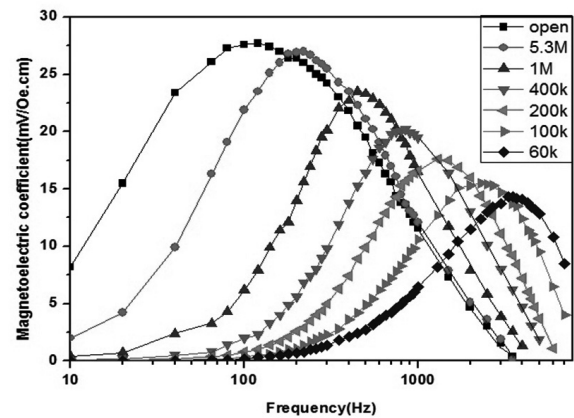


Fig. 7. Frequency dependence of ME coefficient for the 0.2NZFO+0.8PZT ME composite sample at an ac magnetic field of 1 Oe peak, an optimal bias field of 780 Oe, and various load resistances R_L .

This frequency shift effect of R_L shows that the frequency range for the sensor application can be modulated with an appropriate value of R_L .

Fig. 8 shows the ME coefficient and the corresponding ME power as functions of load resistance R_L . The ME coefficient was obtained directly from Fig. 7, and the ME power was calculated by $P = U^2/R_L$ at Hac=1 Oe and $f=100$ Hz. The ME coefficient initially increases with increasing R_L and then seems to be saturated at $R_L > 20$ M Ω .

The ME output power initially increased with increasing load resistance R_L , reached a maximum value 9.3×10^{-10} mW/Oe near $R_L = 3.3$ M Ω , and then decreased with increasing R_L . The maximum output power occurred when the output impedance matched the load impedance as previously mentioned. A similar load resistance influence has been observed in other ME materials [15-17]. Thus, the ME output power of this sample can be adjusted by changing R_L .

Fig. 9(a) and (b) show the output voltage U as a function of the ac magnetic a frequency range of (20~200 Hz) and a load resistance R_L range of (400 k Ω ~ open circuit). The output voltage dependence of the ac field Hac was measured under bias static field Hdc=780 Oe. As clearly shown in Fig. 9(a) and (b), the U has a good linear response to Hac in the measured conditions.

Fig. 9(a) shows that this sample can detect the ac field Hac over the low-frequency range (20~to several hundred Hz). As shown in Fig. 9(b), $dU/dHac$, measured from $R_L = 3.3$ M Ω at the optimal output power condition is approximately 2.5 mV/Oe at Hdc=780 Oe, $f=280$ Hz.

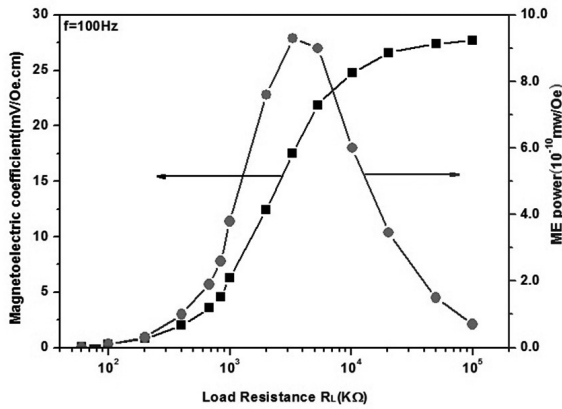


Fig. 8. ME coefficient and ME power as a function of electrical load resistance R_L .

Generally, the ME voltage U depends on the magnitudes of H_{dc} and H_{ac} . This linear characteristic was investigated only for $H_{ac} < 7$ Oe. The measured non-linearity value was approximately 0.8%. This non-linearity value shows that this sample exhibits a good linearity characteristic. This result shows that this sample demonstrates an ability to detect low-strength magnetic ac field in the low-frequency range.

Fig.10 shows the temperature dependence of output voltage U for load resistance $R_L = 5.3$ MΩ, $f = 200$ Hz, and an open-circuit condition, $f = 100$ Hz at $H_{dc} = 780$ Oe and $H_{ac} = 1$ Oe. The dependence was measured for a temperature range of -40 to 80 °C U linearly decreases with increasing temperature and dU/dT is approximately -2.7×10^{-3} mV/°C. From this result, this sample exhibits a fair stability of temperature. This temperature dependence of U is due to the output impedance of the sample material decreasing caused by the temperature increasing [29], and furthermore, the detailed temperature dependence of the materials will be necessary for an analysis of this result.

4. CONCLUSIONS

In this paper, $NiZnF_2O_4 + PZT$ composites were prepared by the conventional ceramic method and the influence of load resistance R_L on the ME characteristics was investigated in the non-resonance frequency range (10 Hz ~ 7 KHz).

The ME coefficient peak increased with increasing R_L , but the frequency indicating the ME coefficient peak decreased with increasing R_L . The ME output power peak

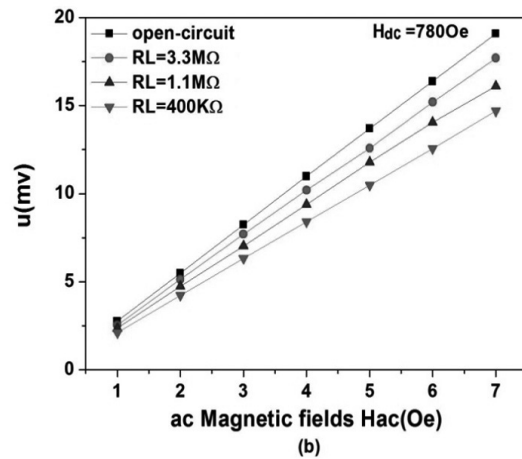
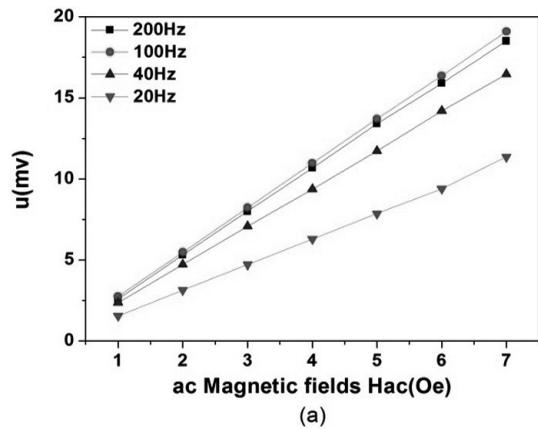


Fig. 9. Output voltage U as a function of the ac magnetic field H_{ac} at (a) various frequencies (open-circuit) and (b) various load resistances R_L and $H_{dc} = 780$ Oe.

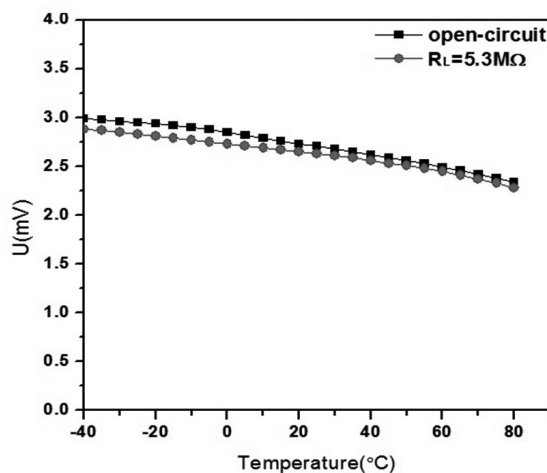


Fig. 10. Temperature dependence of the output voltage U for load resistance $R_L = 5.3$ MΩ and open circuit condition.

was approximately 9.3×10^{-10} mW/Oe near $R_L=3.3 \text{ M}\Omega$ and, $f=280 \text{ Hz}$. However, the ME coefficient seemed to be saturated at $R_L>20 \text{ M}\Omega$. The reason for the frequency shift to a higher frequency and the decrease in the ME coefficient peak due to decreasing R_L can be explained by the impedance matching condition and $f_{\text{cut}}=1/2\pi R_L C$. This frequency shift effect of R_L shows that the frequency range for a sensor application can be modulated with an appropriate value of R_L .

The ME output voltage was almost linearly proportional to the ac field H_{ac} , and dU/dH_{ac} was approximately 2.5 mV/Oe at $H_{\text{dc}}=780 \text{ Oe}$, $f=280 \text{ Hz}$, and $R_L=3.3 \text{ M}\Omega$. The measured non-linearity of this sample was approximately 0.8%. The temperature dependence of the output voltage U showed linear characteristics and dU/dT was approximately $-2.7 \times 10^{-3} \text{ mV}/^\circ\text{C}$

This sample shows good linearity under a low-magnetic ac-field range and a low-frequency range and has a fair stability over temperature. This sample will allow for a low-magnetic ac field sensor. The result from this sample will serve as basic data for a signal-processing circuit system.

ACKNOWLEDGMENT

This work was supported by a Research Grant of Pukyong National University (2013).

REFERENCES

- [1] C. W. Nan, "Magnetoelectric effect in composites of piezoelectric and piezomagnetic phases", *Phys. Rev. B*, Vol. 50, Issue 9, pp. 6082-6088, 1994.
- [2] S. V. Suryanarayana, "Magnetoelectric interaction phenomena in materials", *Bull. Mater. Sci.*, Vol. 17, No. 7, pp. 1259-1270, 1994.
- [3] J. Ryu, S. Priya, K. Uchino, and H. E. Kim, "Magnetoelectric effect in composites of magnetostriction and piezoelectric Materials", *J. Electroceram.*, Vol. 8, pp. 107-119, 2002.
- [4] C. W. Nan, M. I. Bichurin, S. D. Dong, D. Viehland, and G. Srinivasan, "Multiferroic magnetoelectric composites; Historical perspective, status, and future directions", *J. Appl. Phys.*, Vol. 103, Issue 3, pp. 1101-1135, 2008.
- [5] J. Ryu, A. V. Carazo, K. Uchino, and H. Kim, "Piezoelectric and magnetoelectric properties of lead zirconate titanate/Ni-ferrite particulate composites", *J. Electroceram.*, Vol. 7, Issue 1, pp. 17-41, 2001.
- [6] R. A. Islam, D. Viehland, and S. Priya, "Doping effect on magnetoelectric coefficient of $\text{Pb}(\text{Zr}_{0.52}\text{Ti}_{0.48})\text{O}_3\text{-Ni}(1-x)\text{Zn}_x\text{Fe}_2\text{O}_4$ particulate composite", *J. Mater. Sci.*, Vol. 43, pp. 1497-1500, 2008.
- [7] Y. K. Fetisov, K. E. Kamentsev, A. Y. Ostashchenko, and G. Srinivasan, "Wide-band magnetoelectric characterization of a ferrite-piezoelectric multilayer using a pulsed magnetic field", *Solid state Commun.*, Vol. 132, pp. 13-17, 2004.
- [8] D. V. Chashin, Y. K. Fetisov, E. V. Taftseva, and G. Srinivasan, "Magnetoelectric effects in layered samples of lead zirconium titanate and nickel films", *Solid State Commun.*, Vol. 148, pp. 55-58, 2008.
- [9] M. I. Bichurin, D. Viehland, and G. Srinivasan, "Magnetoelectric interactions in ferromagnetic-piezoelectric layered structures; phenomena and devices", *J. Electroceram.*, Vol. 19, pp. 243-250, 2007.
- [10] V. M. Petrov, G. Srinivasan, U. Laletsin, M. I. Bichurin, and D. S. Tuskov, "Magnetoelectric effect in porous ferromagnetic-piezoelectric bulk composites; Experiment and theory", *Phys. Rev. B*, Vol. 75, pp. 174422-174428, 2007.
- [11] A. D. Sheikh, A. Fawzi and V. L. Mathe, "Microstructure-property relationship in magnetoelectric bulk composites", *J. Magn. Magnetic Mater.*, Vol. 323, pp. 740-747, 2011.
- [12] B. K. Bammannavar and L. R. Naik, "Study of magnetic properties and magnetoelectric effect in (x) $\text{Ni}_{0.5}\text{Zn}_{0.5}\text{Fe}_2\text{O}_4+(1-x)$ PZT composites", *J. Magn. Magnetic Mater.*, Vol. 324, pp. 944-948, 2012.
- [13] S. R. Kulkarni, C. M. Kanamadi, and B. K. Chougule, "Dielectric and magnetoelectric properties of (x) $\text{Ni}_{0.8}\text{Co}_{0.1}\text{Cu}_{0.1}\text{Fe}_2\text{O}_4/(1-x)\text{PbZr}_{0.8}\text{Ti}_{0.2}\text{O}_3$ composites", *Mater. Res. Bull.*, Vol. 40, pp. 2064-2072, 2005.
- [14] S. S. Chougule, D. R. Patil, and B. K. Chougule, "Electrical conduction and magnetoelectric effect in ferroelectric rich (x) $\text{Ni}_{0.9}\text{Zn}_{0.1}\text{Fe}_2\text{O}_4+(1-x)$ PZT ME composites", *J. Alloys Compd.*, Vol. 452, pp. 205-209, 2008.
- [15] Y. J. Wang, X. G. Zhao, W. N. Di, H. S. Lu, and S. W. Or, "Magnetoelectric voltage gain effect in a long type magnetostrictive/piezoelectric heterostructure", *Appl. Phys. Lett.*, Vol. 95, p. 143503, 2009.

- [16] Y. J. Wang, X. G. Zhao, J. Jiao, L. H. Liu, W. N. Di, H. S. Luo, and S. Or, "Electrical resistance load effect on magnetoelectric coupling of magnetostrictive / piezoelectric laminate composite", *J. Alloys Compd.*, Vol. 500, pp. 224-226, 2010.
- [17] L. Wang, Z. F. Du, C. F. Fan, L. H. Xu, H. P. Zhang, and D. L. Zhao, "Effect of load resistance on magnetoelectric properties in FeGa/BaTiO₃/FeGa laminate composites", *J. Alloys Compd.*, Vol. 509, pp. 7870-7873, 2011.
- [18] S. T. Chung, K. Nagata, and H. Igarashi, "Piezoelectric and dielectric properties of Pb(Ni,Nb)O₃-Pb(Zn,Nb)O₃-PbZrO₃-PbTiO₃ system ceramics", *Ferroelectrics*, Vol. 94, pp. 243-247, 1989.
- [19] G. Harshe, J. P. Dougherty, and R. E. Newnham, "Magnetoelectric effect in composite materials", *SPIE Proceeding*, Vol. 1919, pp. 224-235, 1993.
- [20] G. Srinivasan, C. P. Devrougd, and C. S. Flattery, "Magnetoelectric interactions in hot-pressed nickle zinc ferrite and lead Zirconate titanate composites", *Appl. Phys. Lett.*, Vol. 85, No. 13, pp. 2550-2552, 2004.
- [21] G. Srinivasan, E. T. Rasmussen, and R. Hayes, "Magnetoelectric effects in ferrite lead zirconate titanate layered composites: The influence of zinc substitution in ferrites", *Phys. Rev. B*, Vol. 67, Issue 1, pp. 014418-014427, 2004.
- [22] R. Grssinger, G.V. Duong, and R. Sato-Turtelli, "The physics of magnetoelectric composites", *J. Magn. Magnetic Mater.*, Vol. 320, pp. 1972-1977, 2008.
- [23] Y. K. Fetisov, A. A. Bush, K. E. Kamentsev, A. Y. Ostaschchenko, and G. Srinivasan, "Ferrite-piezoelectric multilayers for magnetic field sensors", *IEEE Sensor Journal*, Vol. 6, No. 4, pp. 935-938, 2006.
- [24] G. V. Duong, R. Groessinger, M. Schoenhart, and D. Bueno-Nasques, "The lock-in technique for studying magnetielectric effect", *J. Magn. Magnetic Mater.*, Vol. 316, pp. 390-393, 2007.
- [25] S. Dong, J. F. Li, and D. viehland, "Ultra-high magnetic field sensitivity in laminates of Terfenol-D and PMN-PT crystals", *Appl. Phys. Lett.*, Vol. 83, No. 11, pp. 2265-2267, 2003.
- [26] N. H. Duc and D. T. Huong Giang, "Magnetic sensors based on piezoelectric-magnetostrictive composites", *J. Alloys Compd.*, Vol. 449, pp. 214-218, 2008.
- [27] V. M. Petrov, M. I. Bichurin, G. Srinivasan, J. Y. Zhai, and D. Viehland, "Dispersion characteristics for low-frequency magnetoelectric coefficients in bulk ferrite-piezoelectric composite", *Solid State Commun.*, Vol. 142, pp. 515-518, 2007.
- [28] S. Dong, J. Zhai, Z. P. Xing, J. F. Li, and D. Viehland, "Extremely low frequency response of magnetoelectric multilayer composites", *Appl. Phys. Lett.*, Vol. 86, p. 102901, 2005.
- [29] G. Srinivasan, E. T. Rasmussen, A. A. Bush, K. E. Kamentsev, V. F. Meshcheryakov, and Y. K. Fetisov, "Structural and magnetoelectric properties of MFe₂O₄-PZT(M=Ni,Co) and Lax(Ca,Sr)_{1-x}MnO₃-PZT multilayer composites", *Appl. Phys. A*, Vol. 78, pp. 721-728, 2004.